# Acoustical and optical tweezing of bubbles in a microchannel

**G. Memoli[1], C. Fury[1,2], P. Jones[2], E. Stride[3] and B. Zeqiri[1]**

[1]Acoustics Group, National Physical Laboratory, Teddington TW11 8UQ, UK
[2]Department of Physics and Astronomy, University College London, London WC1E 6BT, UK
[3]Institute of Biomedical Engineering, Department of Engineering Science, Headington, Oxford OX3 7DQ, UK

## Introduction

Gas bubbles on the order of 1-10 μm in radius and stabilized by a coating of biological surfactant [1] have found use as contrast agents for ultrasound imaging and, more recently, have shown a clear potential as targeted drug delivery vectors [2].
The characterisation of the acoustic properties of these microbubbles is important in order to validate simulations and improve their design, thereby leading to safer, more clinically effective and cost-effective medical products. In order to perform this characterization at the single bubble level, a system has been constructed based upon simultaneous use of optical and acoustic trapping (NPL "sono-optical tweezers"), with the former providing the reference force calibration and a finer manipulation than the latter.

This study presents a microfluidic system for the acoustical characterisation of microbubbles, based on their simultaneous manipulation through optical and acoustic tweezers.

Characterisation of the acoustic trap is described through the microbubbles' dynamic response to the applied field as monitored by long distance bubble tracking, short scale analysis of the bubble Brownian motion (whilst trapped), high-speed cinematography, laser vibrometry. The changes in the acoustic tweezers with experimental parameters (i.e. driving frequencies and amplitudes) will be observed through measured acoustical pressures in the channel, location of traps and the presence of structural resonances in the device.

## 1. Optical trapping

### *Challenges*

Low relative refractive index objects, such as microbubbles suspended in water, are more challenging to optically trap than high-index particles, as they are strongly repelled from the waist of a focused Gaussian laser beam by both scattering and gradient forces [3]. Microbubble trapping therefore requires alternative strategies.

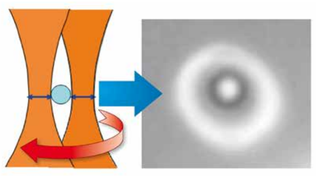

*Scan a focused Gaussian beam around the bubble [3, 4].*

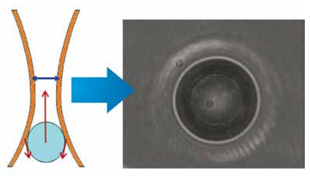

*Use a Laguerre-Gaussian (LG or 'doughnut') beam [5, 6].*

In this study, the optical potential of a microbubble confined in a Laguerre-Gaussian (LG or 'doughnut') beam trap was characterized by determining the transverse spring constant for this geometry in terms of the control parameters: LG topological charge (trap radius) and laser power.

***Measurements:*** Calibration was performed by back focal plane interferometry using the forward scattered light from an additional Gaussian probe laser beam.

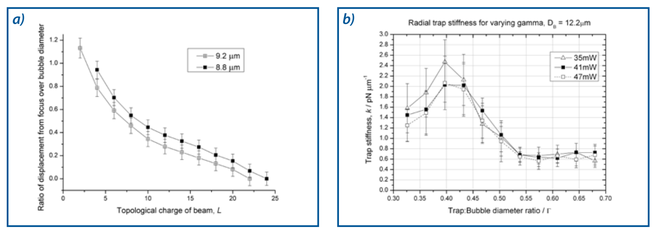


*Figure 1. (a) Vertical displacement of bubble with varying trap diameter, L, (b) Measured radial spring constant normalised by bubble size, a maximum is seen at Γ = 0.4.*

- Changes in the trap diameter cause the bubble to be displaced along the optical axis. As the overlap of the beam onto the bubble surface becomes greater (smaller diameter) the scattering force increases and the equilibrium position against buoyancy is lower.
- Changing the ratio of trap to bubble diameter, Γ, results in a peak in the trap stiffness. This can be seen in *figure 1* b) at Γ = 0.4 for a bubble of diameter 12.2 μm.

## 2. Materials and methods

- Trapping laser: single mode 5W Nd:YAG (Laser Quantum).
- Probe laser: <2mW HeNe (Thorlabs).
- Spatial light modulator (SLM): XY Series, 256x256 pixels (Boulder Non-Linear).
- XY control: a blazed phase grating across the beam.
- Z control: a quadratic (lensing) function ("defocus").
- Objective lens: PLAN APO IR, 60x, 1.27NA, water immersion (Nikon).
- QPD (sampling at 50kHz): bubble position fluctuation measurements in a plane conjugate with the condenser back focal plane (Thorlabs).
- Glass microchannel (0.43x25 mm): enables the bubbles to be manipulated simultaneously with optical and acoustic forces (Dolomite).
- Bubbles: (1) polydisperse polymer coated Expancel 461-WU20, mean diameter 8 μm, range 1 – 40 μm (Akzo Nobel). (2) Filtered size distribution of lipid coated microbubbles, mean diameter 7 μm (University of Oxford).
- Data processing: custom fitting analysis routines (Matlab).
- Bubble fluctuations about the equilibrium position: $\langle x^2 \rangle$ can be related to the spring constant *k* via equipartition of energy [7].
- Pressure measurements: from bubble tracks, as described by Bruus *et al*. [8]

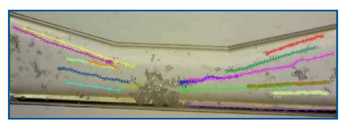

*Figure 2. Video tracking of particles moving under the acoustic force are compared to models of the acoustic field.*

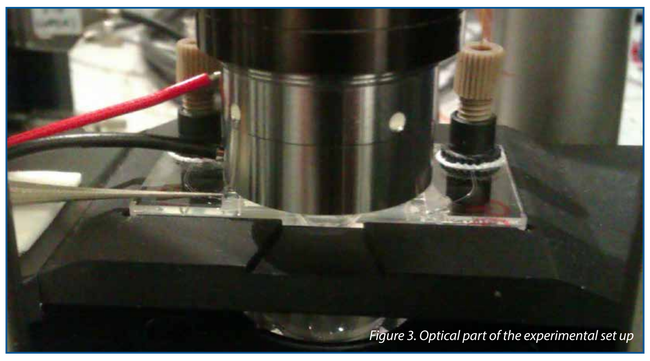

*Figure 3. Optical part of the experimental set up*

## 3. Simultaneous trapping

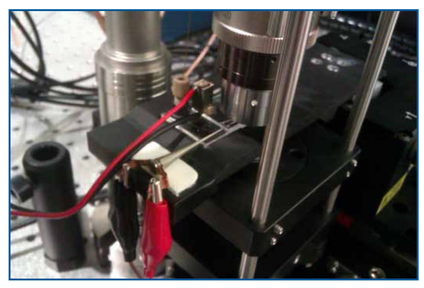

*Figure 4. Acoustic part of the experimental set up.*

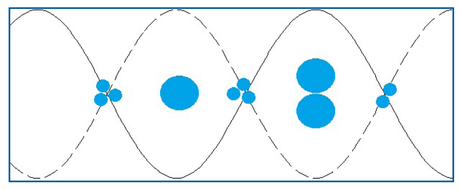

*Figure 5. Bubbles migrate to acoustic nodes or antinodes depending upon their size.*

The pressure gradient within the standing wave aggregates bubbles at the acoustic nodes or anti-nodes. The natural frequency of the bubble dictates to what part of the acoustic field the bubbles move, with an acoustic field higher than the natural frequency causing aggregation at acoustic nodes.

Bubble trapping through acoustic tweezing is both high in force and long ranged. *Figure 6* shows numerous bubbles being collected and trapped from a 4.5 mm region about the acoustic node in 4 seconds.

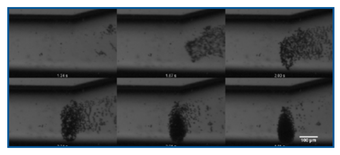

*Figure 6. Acoustic trapping of many microbubbles into an acoustic pressure node. Movie available through QR code.*

Optical tweezers do not possess such high force, and whilst short ranged in comparison they offer good spatial resolution. *Figure 7* shows a bubble, optically trapped, being removed from an acoustic trap like that shown in *figure 4* in ~10 seconds.

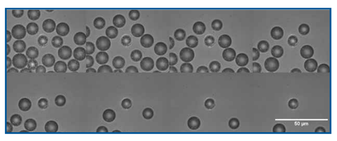

*Figure 7. A single bubble can be extracted from the acoustic trap with the use of optical tweezers. Movie available through QR code.*

## 4. Acoustic characterisation

Image processing of bubble tracks allowed a pressure calibration in the microfluidic chip, in terms of frequency and voltage, so that pressure in the experimental set-up was known within ±10%.

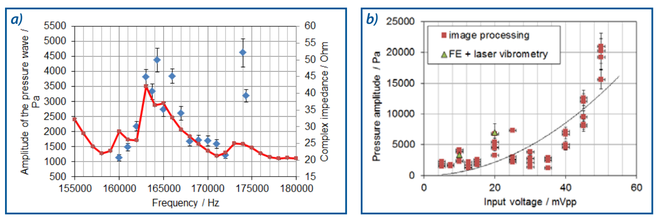


*Figure 8: (a) Pressure and impedance measured as a function of frequency, for 20 mV input voltage. (b) Pressure in the microchannel as a function of input voltage at 164 kHz (standing wave conditions). The triangles show an alternative method to measure pressure, based on FE modelling and laser vibrometry.*

In terms of frequency, data showed good agreement with the input electric impedance, showing that the latter can be used for faster characterisation in the future.

In terms of voltage, dependence was not quadratic, as predicted by simple acoustophoresis. A possible explanation is in the appearance of sub-wavelength structures of bubbles, also appearing in the field of view at some frequencies.

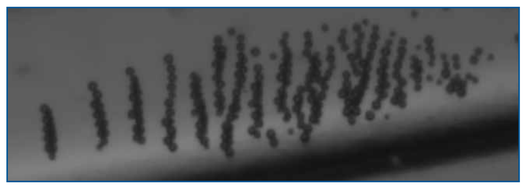

*Figure 9. Sub-wavelength structures at 170 kHz.*

## 5. Acoustic displacement

- Histogramming of bubble position fluctuations with and without acoustic field show a clear displacement in the mean positions.
- Bubble displacement is seen to increase with the drive voltage of the acoustic field, *figure 10 (a)*.

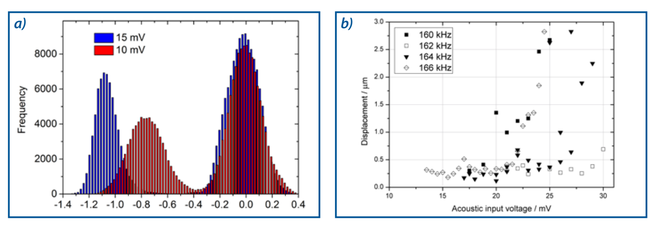


*Figure 10. (a) Position of a 13.8 ± 0.2 μm Expancel under the influence of an acoustic field for two different voltages and for no field. (b) Displacement as a function of frequency with driving voltage for a 9.4 ± 0.2 μm Expancel bubble.*

- Displacement is seen to be a function of frequency, *figure 10(b)*. The device is known to be most efficient at acoustic field generation between 164-165 kHz (*figure 8*), showing a greater bubble displacement as this frequency is approached.

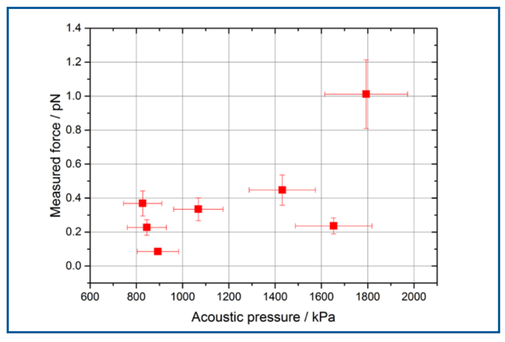


*Figure 11. Acoustic force on the bubble is shown to increase with acoustic field pressure (11 ± 0.2 μm Expancel).*

- Multiplying bubble displacement by the optical trap stiffness reveals the force due to the acoustic field. The force acting on an 11 μm bubble trapped in a Γ = 0.52, 47.3 mW optical trap, 162 kHz, 20mV acoustic trap was found to be 1.0 ± 0.2 pN.

## 6. Soft bubbles

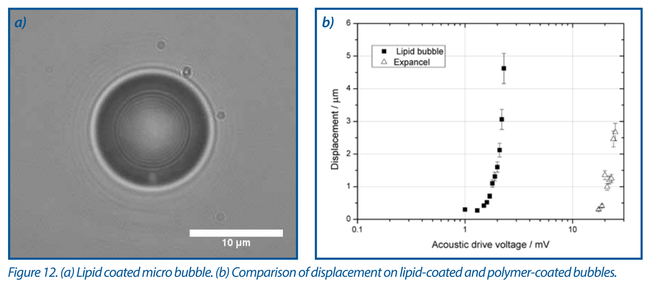


*Figure 12. (a) Lipid coated micro bubble. (b) Comparison of displacement on lipid-coated and polymer-coated bubbles.*

Comparison of the magnitude of displacement with that of Expancel shows that the lipid bubbles are more readily effected by the acoustic field, requiring less acoustic drive to achieve the same displacement, *figure 12*.

## 7. Conclusions

- In this work we demonstrated the simultaneous acoustic and optic manipulation of microbubbles.
- We have investigated the effects of optical trap diameter and laser power on the trap stiffness of the optical trap.
- Bubble tracks were used to measure the pressure in the channel, with a 10% uncertainty. Results were succesfully compared with laser vibrometer data and FE modelling.
- Optical tweezers have been used to calibrate acoustic tweezers, so that the acoustic force on the bubble could be measured.
- Forces on the order of 1pN has been measured on lipid and polymer coated microbubbles.
- The system is sensitive enough to detect displacements due to 0.5% changes in driving frequency, due to different diameters of bubbles and for differing optical trapping conditions such as the trap diameter.

## Acknowledgements

The authors acknowledge financial support from the NPL Strategic Research Fund (project 114248). CF acknowledges additional support from University College London's IMPACT scheme. Thanks are due to Mr. Calvin Tran for helping with the measurements, under a Nuffield Foundation placement.



## References

[1] Hernot, S., Klibanov, A. L., *"Microbubbles in ultrasound-triggered drug and gene delivery,"* Advanced Drug Delivery Reviews, 60, 1153-1166 (2008).
[2] Blomley, M. J. K., Cooke, J. C., Unger, E. C., Monaghan, M. J., Cosgrove, D. O., *"Microbubble contrast agents: a new era in ultrasound,"* BMJ, 322, 1222 (2001).
[3] Jones, P. H. , Stride, E. , Saffari, N., *"Trapping and manipulation of microscopic bubbles with a scanning optical tweezer,"* Appl. Phys. Letters, 89, 081113 (2006).
[4] Jones, P. H., Maragó, O. M., Stride, E. P. J., *"Parametrization of trapping forces on microbubbles in scanning optical tweezers,"* J. of Optics A: Pure & Applied Optics, 9, S278-283 (2007).
[5] Prentice, P. A., MacDonald, M. P., Frank, T. G., Cuschieri, A., Spalding, G. C., Sibbett, W., Campbell, P. A., Dholakia, K. *"Manipulation and fi ltration of low index particles with holographic Laguerre-Gaussian optical trap arrays,"* Optics Express, 12, 593-600 (2004).
[6] Garbin, V. , Cojoc, D. , Ferrari, E., Di Fabrizio, E., Overvelde, M. L. J., van der Meer, S. M., de Jong, N., Lohse, D., Versluis, M., *"Changes in microbubble dynamics near a boundary revealed by combined optical micromanipulation and high-speed imaging,"* Appl Phys Lett, 90, 114103 (2007).
[7] 'Optical tweezers', [Encyclopedia of Optical Engineering], R. G. Driggers & A. W. Hoffman (Eds), Taylor & Francis, New York doi 10.1081/E-EOE-120047157 (2013)
[8] Bruus H. *"Acoustofluidics 7: The acoustic radiation force on small particles"*, Lab Chip, 12, 1014 (2012).
[9] Fury, C., Gélat, P. N., Jones, P. H., Memoli, G., *"Laser vibrometry characterisation of a microfluidic lab-on-a-chip device: a preliminary investigation"*, J. of Physics: Conf. series, 498, 012002 (2014).

www.npl.co.uk